J. Fluid Mech. (1971), *vol.* 46, *part* 4 *pp.* 757–768
Printed in Great Britain

Directional acoustic radiation from a supersonic jet generated by shear layer instability

By CHRISTOPHER K. W. TAM

Department of Aeronautics and Astronautics, Massachusetts Institute of Technology, Cambridge, Massachusetts

(Received 10 February 1970 and in revised form 19 November 1970)

A theory on the generation mechanism of directional acoustic radiation from a supersonic jet is proposed. The theory is based on the concept of instability of the shear layer at the boundary of the jet close to the nozzle. Theoretical prediction of the directional wave pattern is found to agree with shadowgraphic observation.

1. Introduction

Shadowgraphs taken recently on the sound field pattern of a cold supersonic jet (see Lowson & Ollerhead 1968; Dosanjh & Yu 1969) show that strong directional waves are emitted from the shear layer close to the exit of the jet (figure 7), plate 1). On the shadowgraphs these waves appear more or less as parallel straight lines when the jet is operating in its design, shock-free condition. When the jet is operating at an off design condition, i.e. an underexpanded or an overexpanded jet, these waves still appear essentially as straight lines, even though a slight curvature is often noticeable. These waves are found to propagate away from the jet in a downstream direction. In a rather puzzling manner these waves seem to exist only in a limited region of space downstream of the nozzle. They are never found beyond a certain acute angle measured from the jet boundary.

In this paper we wish to propose a theory on the mechanism by which these intense, directional waves are generated. Our proposal is that these waves are the direct consequence of shear layer instability at the jet boundary close to the nozzle. Inside the nozzle it is clear that the flow is full of small disturbances. When these disturbances are convected outside, they become capable of exciting the unstable mode of the shear layer at the boundary of the jet. The instability so excited causes the emission of the directional waves forming the characteristic pattern observed in shadowgraphs.

In the past, the stability of a plane vortex sheet has been studied by Landau (1944), Hatanaka (1949), Pai (1954), Miles (1958) and Fejer & Miles (1963). These authors concluded that under certain conditions a thin shear layer or vortex sheet is unstable. The mathematical theory of vortex sheet instability was rigorously solved by Miles who rejected the spurious roots found by the other authors. Miles obtained a formal solution to the initial-value problem for a plane vortex sheet in an inviscid fluid by means of the transform method. His solution predicts that if the vortex sheet is disturbed by a spatially sinusoidal disturbance

initially, at any fixed point in space, the disturbance will grow exponentially in time in the unstable case. Clearly, this solution is not appropriate for the present jet noise problem. The observed wave pattern does not grow in time. Rather the waves seem to amplify spatially in a downstream direction parallel to the jet boundary until the shear layer is sufficiently thick where the acoustic radiation terminates. In this paper a spatially amplifying wave solution is obtained which is used to compare with experimental results.

The structure of a round underexpanded supersonic jet is rather complicated (see Ollerhead 1969; Adamson & Nicholls 1959). Observations indicate that close to the nozzle exit the jet is bounded by a thin sheet of shear layer. The initial thickness of this layer depends on the boundary-layer thickness inside the nozzle. For a convergent–divergent supersonic nozzle it is usually very thin. The shear layer becomes thicker and thicker in the downstream direction due to intense

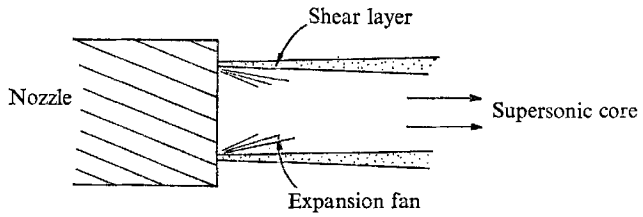

FIGURE 1. Structure of an underexpanded supersonic jet close to the nozzle exit.

mixing of the jet and ambient fluid (figure 1). In the core of the jet the fluid velocity is supersonic but the core size decreases as the mixing layer develops. Right at the end of the nozzle the jet fluid usually undergoes simple expansion until the pressure becomes equal to that of the ambient. A little way downstream three or four jet diameters away, weak shock waves can usually be found. Shadowgraphic observations (see figure 7, plate 1) show that strong unidirectional acoustic waves are emitted from the shear layer close to the nozzle exit. This acoustic radiation terminates somewhere downstream where the shear layer becomes sufficiently thick and usually before the first shock interacts with the shear layer.

To discuss the observed acoustic radiation taking into consideration all the complex flow structures of an underexpanded supersonic jet is beyond the scope of this paper. Here our aim is to examine the generation mechanism of these acoustic waves in relation to the proposed theory. For this purpose we will adopt a simplified model taking into account only the essential details of the jet.

In a supersonic flow as existed near the exit of a nozzle, the effect of compressibility and the inertia of the fluid play a dominant role in the dynamics of the jet. Viscous effects are not very important except in the thin shear layer. As a model for the jet in our proposed theory we will assume that the fluid is inviscid and the thickness of the shear layer infinitesimal. The fluid velocity in the core of the jet will be considered uniform and parallel to the jet axis (see figure 2). The simple expansion which the jet fluid undergoes when leaving the nozzle will be neglected. This approximation is believed to be adequate since the expansion is usually weak unless the jet is operating quite far from its design point. Also from the

observed wavelength of the acoustic radiation one can estimate that only a relatively thin layer of jet fluid adjacent to the shear layer is important in the proposed shear layer instability. The velocity of this layer as a first approximation can be regarded relatively uniform.

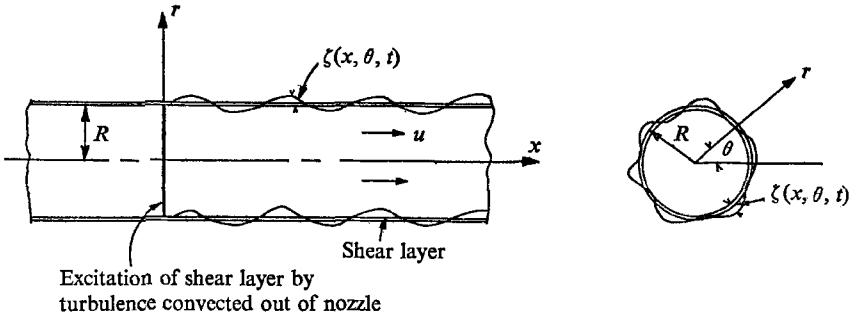

FIGURE 2. Model of a supersonic jet close to the nozzle exit.

It can be shown (following Briggs 1964, chapter 2) that the present shear layer instability is convective in the downstream direction (for a detailed discussion of the concept and properties of convective instability see, for example, Sturrock (1958), and Briggs (1964)). For convective instability the unstable waves propagate away in the downstream direction from the place where they were originally initiated. There is very little upstream influence. Because of this lack of upstream influence on the part of the unstable waves the presence or absence of the nozzle is not at all vital. In fact, the only important function of the nozzle is that it defines where the unstable waves begin. With this in mind, we will, in our simple model, extend the shear layer all the way upstream with the nozzle exit and the excitation of the shear layer by turbulence convected out of the nozzle simulated by a time-dependent pressure fluctuation $f(\theta, t)\,\delta(x)$ located at $x = 0$ as shown in figure 2 (r, θ, x are cylindrical co-ordinates). Without great loss of generality, the pressure fluctuation will be considered as stochastically stationary and quasi-periodic. In this case the function $f(\theta, t)$ can be represented by a double Fourier series,

$$f(\theta, t) = \sum_{n,m} A_{mn}\, e^{i(n\theta - m\nu t)}. \tag{1}$$

In § 2, the mathematical problem of shear layer instability under the influence of a periodic forcing function will be formulated. An asymptotic solution in the sense of long time response is obtained by using the Fourier–Laplace transform method and properly evaluating the poles in the two transform planes. It is found that this solution exhibits all the essential features of the directional wave pattern observed in shadowgraphs of a supersonic jet.

In § 4, we compare the angle between the parallel straight lines formed by wave crests and the shear layer of the jet boundary as given by the theory with the same angle measured on shadowgraphs. Cold nitrogen and cold helium jet shadowgraphs are used. Good agreement is found in both cases. The present theory also predicts that these directional waves are confined to a sector of space downstream of the nozzle exit. The acute angle of this sector calculated from the theory also agrees quite well with the measured angle.

2. Formulation

We consider two ideal fluids occupying the space $r > R$ (R = radius of jet) and $r < R$, designated by the subscripts $+$ and $-$, respectively, as shown in figure 2. We will denote the sonic velocities and fluid densities in these two regions by $a_\pm$ and $\rho_\pm$. The fluid inside the jet will be assumed to have a uniform velocity u parallel to the x axis. The vortex sheet separating the two fluids at the jet boundary is subjected to a localized time and angular dependent sinusoidal disturbance located at $x = 0$. We wish to examine the fluid motion after the sinusoidal disturbance has been introduced for a long time.

On assuming small disturbances, the equations for the perturbation pressures are

$$r > R \qquad \partial^2 p_+/\partial t^2 = a_+^2 \nabla^2 p_+; \tag{2}$$

$$r < R \qquad \left(\frac{\partial}{\partial t} + u\frac{\partial}{\partial x}\right)^2 p_- = a_-^2 \nabla^2 p_-. \tag{3}$$

The dynamic and kinematic boundary conditions at the vortex sheet $r = R + \zeta(x, \theta, t)$ are

$$r = R \qquad -\frac{1}{\rho_+}\frac{\partial p_+}{\partial r} = \frac{\partial^2 \zeta}{\partial t^2}; \quad -\frac{1}{\rho_-}\frac{\partial p_-}{\partial r} = \left(\frac{\partial}{\partial t} + u\frac{\partial}{\partial x}\right)^2 \zeta, \tag{4}$$

$$p_+ = p_- + A\, e^{i(n\theta - \nu t)}. \tag{5}$$

Other boundary conditions are

$$p_- \text{ is finite} \quad \text{as} \quad r \to 0, \tag{6}$$

$$p_+ \to 0 \quad \text{as} \quad r \to \infty \text{ for finite } t. \tag{7}$$

In (5) only one Fourier component of (1) is included. This is permissible since the problem is linear. Other components can be accounted for by superposition. Without loss of generality the frequency ν in (5) will be assumed to be positive. Further, we will make the simplifying assumption that the specific heat ratios of the two fluids are equal so that from the condition of equilibrium at the unperturbed state we have

$$\rho_+ a_+^2 = \rho_- a_-^2. \tag{8}$$

(The general case when the specific heat ratios of the two fluids are different can be extended in a straightforward manner.)

We propose to solve the above problem by the method of the Fourier–Laplace transform. We define $P_\pm$, the Fourier–Laplace transform of $p_\pm$, as

$$\left.\begin{aligned} P_\pm e^{in\theta} &= \int_0^\infty \int_{-\infty}^\infty p_\pm e^{-i(kx-\omega t)}\, dx\, dt, \\ p_\pm &= \frac{1}{4\pi^2}\int_{-\infty+i\sigma}^{+\infty+i\sigma}\int_{-\infty}^{+\infty} P_\pm e^{i(kx-\omega t+n\theta)}\, dk\, d\omega. \end{aligned}\right\} \tag{9}$$

On applying the Fourier–Laplace transform to (2)–(7), a straightforward calculation gives

$$P_+ = \frac{iA\Omega^2 \xi_- J_n'(\xi_-) H_n^{(1)}(\xi_+ r/R)/(\omega - \nu)}{\Omega^2 \xi_- J_n'(\xi_-) H_n^{(1)}(\xi_+) - \left(\frac{a_+}{a_-}\right)^2 \left(\Omega - \frac{u}{a_+}\lambda\right)^2 \xi_+ J_n(\xi_-) \frac{d}{d\xi_+} H_n^{(1)}(\xi_+)}, \tag{10}$$

where $$\Omega = \omega R/a_+, \qquad \lambda = kR,$$

$$\xi_+ = (\Omega^2 - \lambda^2)^{\frac{1}{2}}, \quad \xi_- = \left[\frac{a_+^2}{a_-^2}\left(\Omega - \frac{u}{a_+}\lambda\right)^2 - \lambda^2\right]^{\frac{1}{2}}; \quad \mathrm{Im}\,(\xi_\pm) > 0.$$

J_n and $H_n^{(1)}$ are the Bessel and Hankel function of the first kind, respectively,

$$J_n'(\xi) = dJ_n(\xi)/d\xi.$$

In obtaining (10) we have put all the initial conditions equal to zero. In the present problem any initial disturbances (including those that are unstable) will be convected away and, therefore, they are unimportant as far as the long-time response is concerned.

3. An asymptotic solution

A complete study of (10), as obtained in the above section, is rather lengthy and will not be reproduced here (extensive numerical work is necessary). Instead, we observe from shadowgraphs that the relevant wavelengths of the directional acoustic wave are very small compared to the radius of the jet. That is to say, the corresponding value of $|\lambda|$ in (10) is extremely large. For large values of $|\lambda|$, the following asymptotic formula for J_n and $H_n^{(1)}$ are available.

$$\left.\begin{aligned} J_n(\xi_-) &\sim \frac{1}{(2\pi\xi_-)^{\frac{1}{2}}}\exp\{-i(\xi_- - \tfrac{1}{2}n\pi - \tfrac{1}{4}\pi)\}, \\ H_n^{(1)}(\xi_+) &\sim \left(\frac{2}{\pi\xi_+}\right)^{\frac{1}{2}}\exp\{i(\xi_+ - \tfrac{1}{2}n\pi - \tfrac{1}{4}\pi)\}, \\ &\mathrm{Im}\,(\xi_\pm) > 0. \end{aligned}\right\} \tag{11}$$

On substituting (11) into (10), we find

$$P_+ \sim \frac{iAc^2\beta_- e^{ik\beta_+(r-R)}}{(\beta_+ + \beta_-)(\beta_+\beta_- + 1)(\omega - \nu)}, \tag{12}$$

where

$$c = \omega/ka_+, \quad \beta_+(c) = (c^2-1)^{\frac{1}{2}}, \quad \beta_-(c) = \left[\left(\frac{a_+}{a_-}\right)^2\left(c - \frac{u}{a_+}\right)^2 - 1\right]^{\frac{1}{2}}; \quad \mathrm{Im}(\beta_\pm) > 0.$$

In what follows we will use the asymptotic expression of (12) instead of (10). Physically this means that we consider only the contributions of the short waves. The long waves are important in other phenomena of the jet involving scale lengths of the order of the jet diameter. In the present physical problem they are not so relevant. Mathematically (12) amounts to retaining only the leading term of an asymptotic expansion of (10). The neglected terms are of the order of $(1/|\lambda|)$.

From (12) and (9) the pressure distribution for $r > R$ is given by

$$p_+ = \frac{iA}{4\pi^2}\int_{-\infty+i\sigma}^{+\infty+i\sigma} G(\omega; x, r)\frac{e^{i(n\beta-\omega t)}}{(\omega-\nu)}\,d\omega, \tag{13}$$

$$G(\omega; x, r) = \int_{-\infty}^{+\infty} \frac{\beta_- c^2}{(\beta_+ + \beta_-)(\beta_+\beta_- + 1)} e^{ik(x+\beta_+(r-R))}\,dk. \tag{14}$$

The poles of the integrand in (14) have been studied by Miles (1958) who concluded that: (*a*) the vortex sheet is unstable if $u < (a_+^{\frac{2}{3}} + a_-^{\frac{2}{3}})^{\frac{3}{2}}$; (*b*) the function

$(\beta_+(c)+\beta_-(c))$ has no complex zeros and hence does not give rise to unstable poles; (c) in the unstable case, the zeros of the function $(\beta_+(c)\beta_-(c)+1)$ are the two complex conjugate roots of $(\beta_+^2\beta_-^2-1)$, i.e. the complex solutions of

$$F(c) \equiv c^4 - 2\left(\frac{u}{a_+}\right)c^3 + \left[\left(\frac{u}{a_+}\right)^2 - \left(\frac{a_-}{a_+}\right)^2 - 1\right]c^2 + 2\left(\frac{u}{a_+}\right)c - \left(\frac{u}{a_+}\right)^2 = 0. \quad (15)$$

The two roots of $(\beta_+\beta_- - 1)$ are real.

Let us denote the two complex roots of (15) by

$$c_\pm = c_r \pm ic_i \quad (c_i > 0), \quad (16)$$

and the corresponding value of $\beta_+(c_+)$ by

$$\beta_+(c_+) = \beta_r + i\beta_i \quad (\beta_i > 0). \quad (17)$$

We note that $c_\pm$ are constants depending only on the parameters a_-/a_+ and u/a_+.

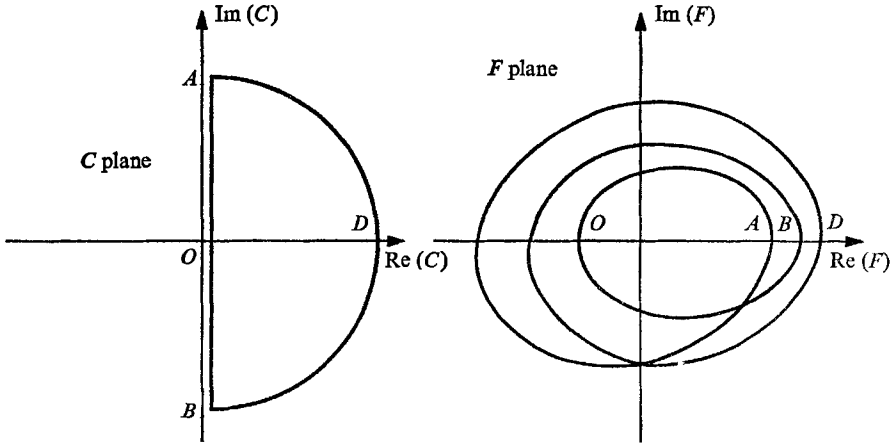

FIGURE 3. Mapping of left half c plane on the F plane.

By mapping the function $F(c)$ along the contour $AOBD$ as shown in figure 3 in the c plane, we see that the corresponding contour in the F plane encircles the origin three times. Hence three of the roots of $F(c)$ have positive real parts. This implies that c_r in (16) is positive.

In this paper we will assume that $u < (a_+^{\frac{2}{3}} + a_-^{\frac{2}{3}})^{\frac{3}{2}}$, so that the vortex sheet is unstable. Now let us evaluate integrals (13) and (14) asymptotically for large t.† In the past, some confusion arises as to how the contours in the complex ω and k planes of these integrals should be deformed in relation to the poles of the integrand. This problem was examined by Briggs (1964, chapter 2) and a correct procedure was given by him. In this paper we will follow his method. Let us choose initially a contour with $\mathrm{Im}\,(\omega) \to +\infty$ for the integral in (13) and slowly deform it towards the real axis in the ω-plane (see Briggs 1964, chapter 2) as shown in figure 4. In the k plane, the poles of the integrand in (10) are related to c and ω by

$$k^\pm = \frac{\omega}{c_\pm a_+} = \{(\omega_r c_r \pm \omega_i c_i) + i(\omega_i c_r \mp \omega_r c_i)\}\frac{1}{(c_r^2 + c_i^2)a_+}, \quad (18)$$

where $\omega = \omega_r + i\omega_i$.

† An alternative way of evaluating these integrals was suggested by a referee which also led to the same results as obtained below.

If we let $\omega_r = \nu$, we have

$$\text{as} \quad \omega_i \to \infty, \quad \mathrm{Re}\{k^{\pm}\} \to \pm\infty, \quad \mathrm{Im}\{k^{\pm}\} \to \infty;$$

$$\text{as} \quad \omega_i \to 0, \quad \begin{cases} \mathrm{Re}\{k^{+}\} \to \dfrac{\nu c_r}{(c_r^2+c_i^2)a_+}, & \mathrm{Im}\{k^{+}\} \to -\dfrac{\nu c_i}{(c_r^2+c_i^2)a_+}; \\ \mathrm{Re}\{k^{-}\} \to \dfrac{\nu c_r}{(c_r^2+c_i^2)a_+}, & \mathrm{Im}\{k^{-}\} \to +\dfrac{\nu c_i}{(c_r^2+c_i^2)a_+}. \end{cases}$$

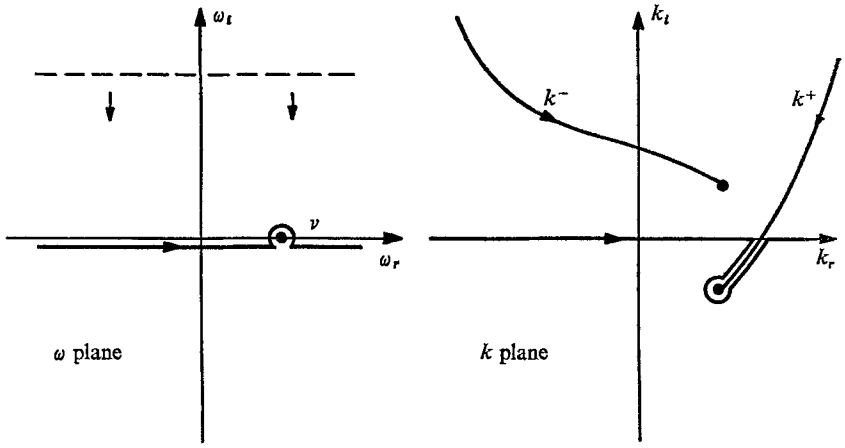

FIGURE 4. Inversion contours in the ω and k planes.

Therefore, the two poles, $k^{\pm}$, lie in the upper half k plane originally. As the inversion contour in the ω plane is being pushed towards the real axis, the contour in the k plane must be deformed so that it remains below the two poles as shown in figure 4. This is required since the integral will become undefined if a pole crosses the inversion contour in the k plane. As $t \to \infty$, the dominant contribution to (13) and (14) comes from the pole $\omega = \nu$ in the ω plane and the pole $k = k^{+}$ in the k plane; k^{+} is the pole which moves below the real k axis. The contributions from the other pole, etc., will be neglected as they do not give rise to amplifying waves. Thus on completing the contours of integration by adding appropriate large semicircular paths in the upper or lower half plane, we obtain asymptotically

$$p_+(x,r,\theta,t) \underset{t\to\infty}{\sim} \left\{ \begin{array}{ll} \dfrac{iA\nu\beta_- c_+^2}{a_+(\beta_+ + \beta_-)\, d(\beta_+\beta_-)/dc} \exp\left\{ i\left[\dfrac{x}{c_+} + \dfrac{\beta_+}{c_+}(r-R) - a_+ t\right]\dfrac{\nu}{a_+} + in\theta \right\} & \\ & (x > 0), \\ 0 & (x < 0); \end{array} \right\}$$

$$\text{or} \quad \sim \left\{ \begin{array}{ll} \text{const.} \exp\left\{ \dfrac{c_i x - (c_r\beta_i - c_i\beta_r)(r-R)}{c_r^2 + c_i^2} \dfrac{\nu}{a_+} \right\} & \\ \quad \times \exp\left\{ i\left[\dfrac{c_r x + (c_r\beta_r + c_i\beta_i)(r-R)}{c_r^2+c_i^2} - a_+ t \right]\dfrac{\nu}{a_+} + in\theta \right\} & (x > 0); \\ 0 & (x < 0). \end{array} \right\} \tag{19}$$

The amplifying wave solution (19) shows that the disturbance consists of a spatially dependent amplitude and a wave-like oscillatory part. The disturbance is exponentially small to the left of the line.

$$c_i x - (c_r\beta_i - c_i\beta_r)(r-R) = 0 \tag{20}$$

as shown in figure 5. This line makes an angle ϕ with the x axis, the tangent of which is given by

$$\tan\phi = c_i/(c_r\beta_i - c_i\beta_r). \tag{21}$$

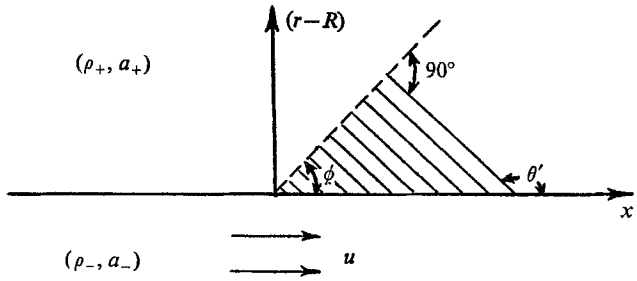

FIGURE 5. Pattern of acoustic disturbance.

The amplifying wave solution grows exponentially in the x direction. When the amplitude becomes sufficiently large, non-linear effects can no longer be neglected and the present solution does not apply. However, because of the lack of upstream influence in a convective instability the present theory is meaningful for small values of x, i.e. close to the nozzle exit.

Further, on a plane θ = constant (or in the case $n = 0$) the disturbance consists of wave crests and troughs which are straight lines. These straight lines are given by the equation

$$c_r x + (c_r\beta_r + c_i\beta_i)(r-R) - a_+(c_r^2 + c_i^2)t = \text{constant}. \tag{22}$$

The slope of these parallel lines is

$$\tan\theta' = -c_r/(c_r\beta_r + c_i\beta_i) \tag{23}$$

as shown in figure 6. In appendix A, it will be shown that

$$\theta + \phi = \tfrac{1}{2}\pi, \quad \theta = \pi - \theta'. \tag{24}$$

From (22), the velocity of these lines (on a plane θ = constant) is found to be

$$v = \frac{a_+(c_r^2 + c_i^2)}{[c_r^2 + (c_r\beta_r + c_i\beta_i)^2]^{\frac{1}{2}}}. \tag{25}$$

This velocity is, in general, unequal to the sound speed a_+. This seems to be a rather strange result especially in the case $n = 0$. To understand this puzzling phenomenon one must bear in mind that we are dealing with unstable waves. From previous results on the propagation properties of unstable waves (see Tam 1967; Briggs 1964) it is known that the motion of the wave front of unstable waves is strongly influenced by the growth rate. This is what happens in the present problem. In order to demonstrate that unstable waves do not always propagate with the speed of sound, we carry out further some calculations on the

initial-value problem of an unstable vortex sheet set in motion by a sinusoidal initial disturbance considered by Miles (1958) in appendix B. It is shown that in this problem the lines of constant phase also do not, in general, propagate with the velocity of sound a_+. So the result (25) is not to be viewed with suspicion. Actually, it offers a means of verifying the proposed instability theory experimentally.

4. Comparison with experiments

Shadowgraphs of noise pattern from cold supersonic jets are available in published form (Ollerhead 1966; Lowson & Ollerhead 1968; Dosanjh & Yu 1969). In this section we want to compare the directional waves observed in these shadowgraphs with directional waves predicted in the previous section by assuming that these waves are generated by shear layer instability at the jet boundary. In the analysis above, the calculation was carried out for a jet of

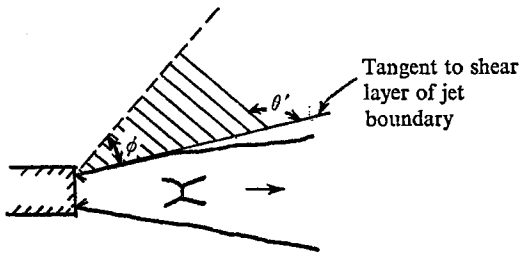

FIGURE 6. Angular measurements for an underexpanded jet.

constant radius. However, for an underexpanded or an overexpanded jet, the jet boundary near the nozzle exit is slightly curved, i.e. R is not a constant. In order to compare theory and experiment we will measure all relevant angles of the disturbance pattern not relative to the jet axis, but rather from the tangent to the jet boundary as shown in figure 6. We note from these shadowgraphs that when the jet boundary is sufficiently curved, the directional waves are no longer very straight. We believe that an improved analysis based on a curved vortex layer could account for this effect.

Good-quality shadowgraphs taken by Ollerhead (1966) are available as figure 19 in a report by Potter (1968). Table 1 is a comparison of the observed angles, θ and ϕ and the angles as calculated by equations (21) and (23).

It is clear from table 1 that there is good agreement between theory and experimental results.

The above experimental data were obtained from a cold nitrogen jet. But in practice, e.g. the jet of an aircraft, the jet is hot. A hot jet has the properties that the density of the jet fluid is less than that of the ambient while the speed of sound is greater than that of air outside. To simulate a hot jet and to further verify the above theory we carried out a series of experiments using a helium jet. Helium has lower density and higher sound speed than air and is therefore ideal to use. In our experiment a spark source with a life time of $\frac{1}{3}\,\mu$sec was used. The

experimental procedure employed was similar to that of Lowson & Ollerhead (1968) and will therefore not be described. Figure 7 (plate 1) is a typical shadowgraph showing the sound field of a supersonic helium jet obtained. Since helium and air have different specific heat ratios, the above analysis was extended to account for this effect. Table 2 shows a comparison of theoretical and experimental results. Again, there is good agreement between theory and experimental results.

				θ		ϕ		
Case	P_E/P_0	a_-/a_+	u/a_+	Observed	Calculated	Observed	Calculated	Observed, $\theta+\phi$
1	1	0·671	1·658	50°	50° 4′	40°	39° 55′	90°
2	1·53	0·630	1·736	51°	50° 40′	38°	39° 20′	89°
3	1·98	0·608	1·775	51°	50° 48′	38°	39° 12′	89°

Note. (i) Values of a_-/a_+ and u/a_+ are calculated by assuming isentropic expansion from ambient stagnation temperature: see Lowson & Ollerhead (1968). (ii) The observed angles have an uncertainty of 2–3°.

TABLE 1. Nitrogen jet

				θ		ϕ		
Case	P_t Psia	a_-/a_+	u/a_+	Observed	Calculated	Observed	Calculated	Observed $\theta+\phi$
1	54·7	2·259	3·253	35°	33° 39′	54°	56° 21′	89°
2	74·7	2·122	3·518	33°	34° 1′	59°	55° 59′	92°
3	104·7	1·984	3·753	33°	33° 16′	58°	56° 44′	91°
4	114·7	1·948	3·809	32°	32° 51′	59°	57° 9′	91°

(P_t = chamber pressure)

TABLE 2. Helium jet

To conclude, we believe that the directional sound waves radiated from the shear layer of a supersonic jet is the direct result of instability of the shear layer. Experimental results are found to confirm the overall acoustic field pattern predicted by the theory of instability. Based on the present results, it seems likely that acoustic radiation can also be generated by instabilities under similar conditions in wakes and possibly even in boundary layers. Further work on this area is desirable.

The author wishes to thank Mr Arturo Rosales for his assistance in the experimental part of this paper. Part of this work was supported by NASA under Grant NGL 22-009-383.

Appendix A

In this appendix we want to show that $\theta+\phi=\frac{1}{2}\pi$. From (12) we have

$$\beta_+^2(c_+)=c_+^2-1. \tag{A 1}$$

By equating real and imaginary parts we obtain

$$\beta_r\beta_i=c_rc_i, \tag{A 2}$$

$$\beta_r^2-\beta_i^2=c_r^2-c_i^2-1. \tag{A 3}$$

By means of (A 2) and (A 3), it is straightforward to show from (21) and (23) that

$$\tan\theta'\tan\phi=-1,$$

and hence $\theta+\phi=\frac{1}{2}\pi$.

Appendix B

Miles (1958) considered an initial-value problem of a vortex sheet set in motion by an initial sinusoidal disturbance. Here we want to complete his analysis by obtaining the pressure field and to show that the lines of constant phase for the unstable wave do not propagate in general with the speed of sound as found also in the present problem (25). For the purpose of illustrating this point we will assume

$$u_+=0, \quad u_-=u, \quad \rho_+a_+^2=\rho_-a_-^2 \quad (u \text{ is in the unstable range}).$$

From equation (4.8) of Miles's paper we find that the pressure in the region above the vortex sheet is given by (the notation of Miles is used)

$$p_+=-\frac{\rho_-uv_0}{2\pi ia_+^2}\int_{-\infty+i\epsilon}^{\infty+i\epsilon}\frac{(2c-u)\,e^{i\alpha(x-ct+\beta_+y)}}{(\beta_++\beta_-)(\beta_+\beta_-+1)}dc. \tag{B 1}$$

The poles and branch cuts of the integrand of (B 1) are similar to that given in figure 8 of Miles's paper. For large time, the contribution from the unstable pole dominates, hence on deforming the contour as Miles did, we obtain

$$\begin{aligned}p_+(x,y,t)\underset{t\to\infty}{\sim}&\frac{\rho_-uv_0(2c_+-u)}{a_+^2(\beta_++\beta_-)\,d(\beta_+\beta_-)/dc}\,e^{i\alpha(x+\beta_+y-c_+t)}\\&+\text{contributions from branch cuts and damped pole;}\\\sim&\ \text{constant}\ e^{i\alpha(x+\beta_ry-c_rt)}\,e^{(c_it-\beta_iy)},\end{aligned}$$

$$c_+=c_r+ic_i, \quad \beta_+=\beta_r+i\beta_i.$$

Lines of constant phase are given by

$$x+\beta_ry-c_rt=\text{constant}.$$

These lines propagate with velocity

$$v=\frac{c_r}{(1+\beta_r^2)^{\frac{1}{2}}},$$

which is, in general, unequal to a_+. In Miles's problem the unstable wave covers the region $-\infty<x<\infty$ and is therefore slightly different from the jet noise problem considered above.

REFERENCES

ADAMSON, T. C. & NICHOLLS, J. A. 1959 On the structure of jets from highly underexpanded nozzles into still air. *J. Aerospace Sci.* **26**, 16.

BRIGGS, R. J. 1964 *Electron Stream Interactions with Plasmas*. MIT Press.

DOSANJH, D. S. & YU, J. C. 1969 Noise from underexpanded axisymmetric jet flows using radial jet flow impingement. *Proceedings of AFOSR-UTIAS Symposium*, May 1968, Toronto.

FEJER, J. A. & MILES, J. W. 1963 On the stability of a plane vortex sheet with respect to three-dimensional disturbances. *J. Fluid Mech.* **15**, 335.

HATANAKA, H. 1949 Stability of tangential discontinuities in a compressible fluid. *J. Soc. Sci. Culture, Japan*, **2**, 3.

LANDAU, L. 1944 Stability of tangential discontinuities in a compressible fluid. *Akademia Nauk, SSSR. Comptas.*

LOWSON, M. V. & OLLERHEAD, J. B. 1968 Visualization of noise from cold supersonic jets. *J. Acoustic Soc. Am.* **44**, 624.

MILES, J. W. 1958 On the disturbed motion of a plane vortex sheet. *J. Fluid Mech.* **4**, 538.

OLLERHEAD, J. B. 1966 Some shadowgraph experiments with a cold supersonic jet. *Wyle Res. Rep.* WR 66-44.

OLLERHEAD, J. B. 1969 On the prediction of the near field noise of supersonic jets. *NASA* CR 857.

PAI, S. I. 1954 On the stability of a vortex sheet in an inviscid compressible fluid. *J. Aero. Sci.* **21**, 325.

POTTER, R. C. 1968 An investigation to locate the acoustic sources in a high speed jet exhaust stream. *Wyle Lab. Res. Staff Tech. Rep.* WR 68-4.

STURROCK, R. C. 1958 Kinematics of growing waves. *Phys. Rev.* **112**, 1488.

TAM, C. K. W. 1967 A note on disturbances in slightly supercritical plane Poiseuille flow. *J. Fluid Mech.* **30**, 17.

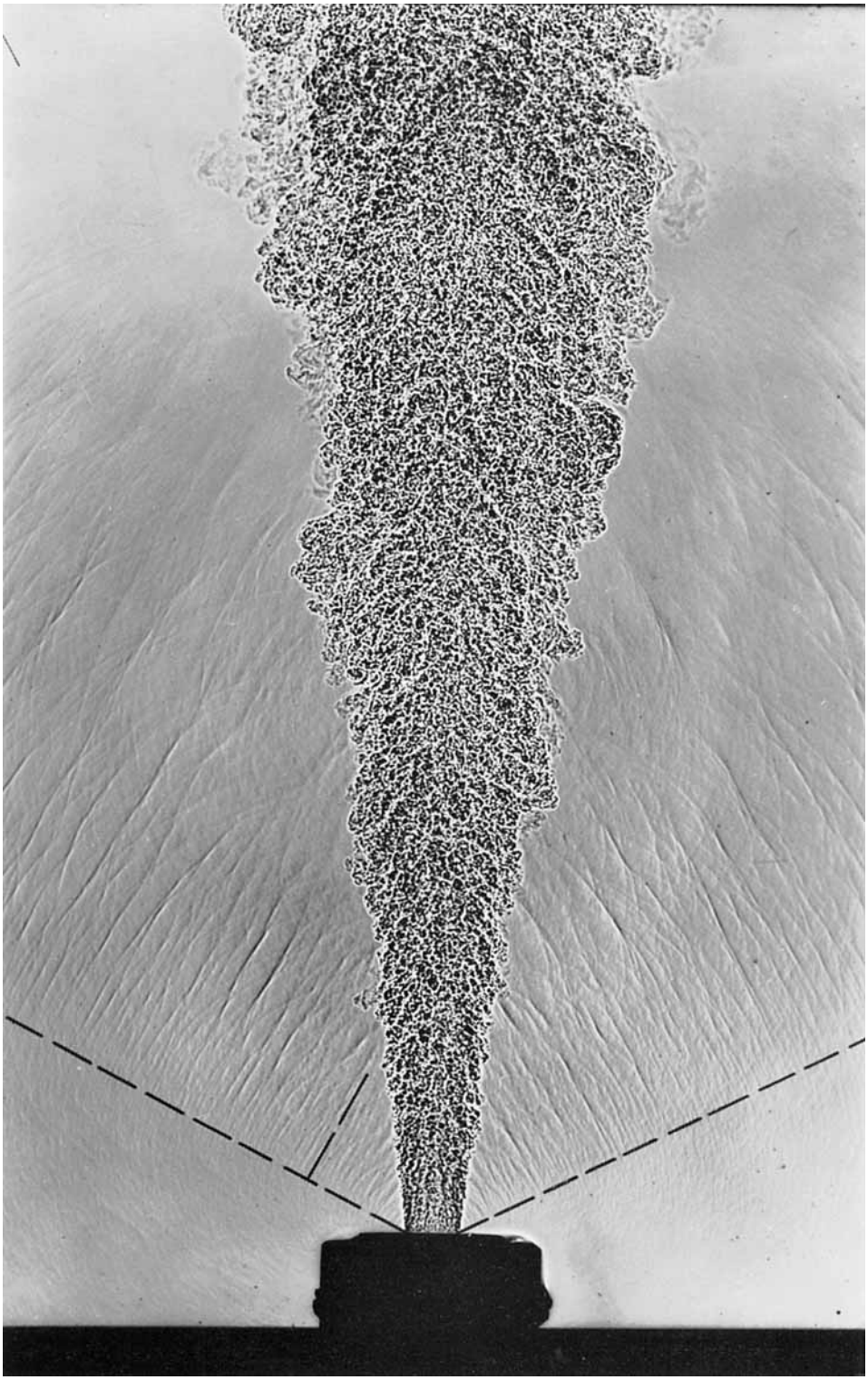

FIGURE 7. Helium jet (P_t = 54·7 psia).

(*Facing p.* 768)